

# Implementing geomechanical models in MFront/OpenGeoSys for hydrogeological and geotechnical applications

Christian B. Silbermann<sup>1</sup>, Dominik Kern<sup>1</sup>, Francesco Parisio<sup>1</sup>, Dmitri Naumov<sup>1</sup>, Thomas Nagel<sup>1,3</sup>

<sup>1</sup> Institute of Geotechnics, Technische Universität Bergakademie Freiberg

<sup>3</sup> TUBAF-UFZ Centre for Environmental Geosciences

More:

<https://tu-freiberg.de/en/soilmechanics>

## INTRODUCTION

- proper simulation of complex hydrogeological or geotechnical processes
- reasonably capture the mechanical behavior of the geomaterials!
- constitutive relation for the calculation of the effective stress tensor
- part of the constitutive closing of the thermo-hydro-mechanical theory
- variety of inelastic thermo-mechanical (geo)material models available in literature

### Goal of this talk

Highlight recent implementations of geo-mechanical models in *MFront/OpenGeoSys*, such as:

- \* rock mechanical models depending on temperature and pressure,  
spanning the brittle-ductile transition
- \* models for primary, secondary and tertiary creep of rock salt
- \* models for fine-grained soils

## INTRODUCTION

- proper simulation of complex hydrogeological or geotechnical processes
- reasonably capture the mechanical behavior of the geomaterials!
- constitutive relation for the calculation of the effective stress tensor
- part of the constitutive closing of the thermo-hydro-mechanical theory
- variety of inelastic thermo-mechanical (geo)material models available in literature

### Goal of this talk

Highlight recent implementations of geo-mechanical models in *MFront/OpenGeoSys*, such as:

- \* rock mechanical models depending on temperature and pressure,  
spanning the brittle-ductile transition
- \* models for primary, secondary and tertiary creep of rock salt
- \* models for fine-grained soils

## OUTLINE

Importance of elasto-plastic material models in geoscience

Coupling of OpenGeoSys and MFront

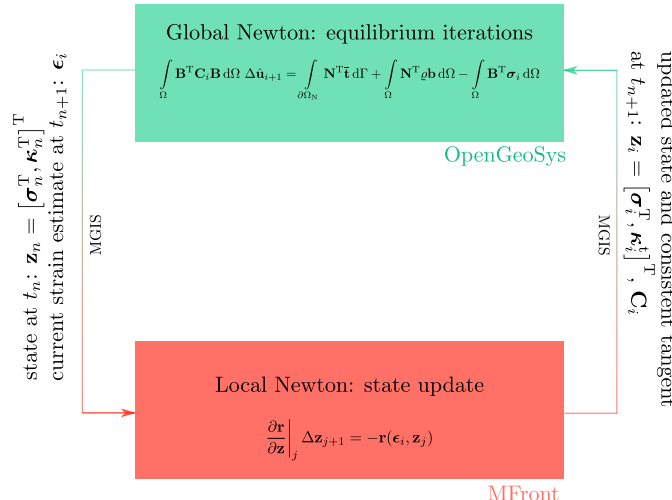
Brittle-ductile transition model

Dislocation and pressure-solution creep model

Günther-Salzer model with damage

Modified Cam clay model

## GLOBAL AND LOCAL NEWTON-RAPHSON PROCEDURES



# CONSTITUTIVE EQUATIONS AND INTERPRETATION

## Basic equations:

$$\boldsymbol{\epsilon} = \boldsymbol{\epsilon}^e + \boldsymbol{\epsilon}^p + \boldsymbol{\epsilon}^v + \boldsymbol{\epsilon}^{th} \quad \text{with} \quad \boldsymbol{\epsilon}^{th} = \alpha_T \Delta T \mathbf{I}$$

$$\tilde{\boldsymbol{\sigma}} = \boldsymbol{\sigma} / (1 - d) = K (\operatorname{tr} \boldsymbol{\epsilon}^e) \mathbf{I} + 2G \boldsymbol{\epsilon}_D^e$$

$$\frac{d\boldsymbol{\epsilon}^v}{dt} = \sqrt{\frac{3}{2}} A \exp\left(-\frac{Q}{RT}\right) \left(\frac{\tilde{\boldsymbol{\sigma}}_D}{\sigma_{ref}}\right)^m \frac{\tilde{\boldsymbol{\sigma}}_D}{\|\boldsymbol{\sigma}_D\|}$$

$$\frac{d\boldsymbol{\epsilon}^p}{dt} = \lambda^p \frac{\partial g^p}{\partial \tilde{\boldsymbol{\sigma}}}$$

$$f^p = \left[ (1-q_h) \left( \frac{\tilde{\boldsymbol{\sigma}}_D}{3\sigma_c} + \frac{\tilde{\boldsymbol{\sigma}}_m}{\sigma_c} \right)^2 + \frac{\tilde{\boldsymbol{\sigma}}_D}{\sigma_c} \right]^2 + m_0 q_h^2 \left( \frac{\tilde{\boldsymbol{\sigma}}_D}{3\sigma_c} + \frac{\tilde{\boldsymbol{\sigma}}_m}{\sigma_c} \right) - q_h^2$$

$$q_h = \frac{R_p(\boldsymbol{\epsilon}^p, \boldsymbol{\epsilon}^v)}{[1 + (\alpha \Delta T)^n]^{(1-\frac{1}{n})}}, \quad \tilde{\boldsymbol{\sigma}}_m = \frac{1}{3} \operatorname{tr}(\tilde{\boldsymbol{\sigma}}), \quad \tilde{\boldsymbol{\sigma}}_D = \sqrt{\frac{3}{2} \tilde{\boldsymbol{\sigma}}_D : \tilde{\boldsymbol{\sigma}}_D}$$

cf. Parisio, Lehmann und Nagel 2020

## Captured effects/phenomena:

- elastic-plastic model with yield surface
- scalar internal damage variable  $d$
- temperature-dependent Young modulus
- Norton creep law with Arrhenius term

# CONSTITUTIVE EQUATIONS AND INTERPRETATION

**Basic equations:**

$$\epsilon = \epsilon^e + \epsilon^p + \epsilon^v + \epsilon^{th} \quad \text{with} \quad \epsilon^{th} = \alpha_T \Delta T \mathbf{I}$$

$$\tilde{\sigma} = \sigma / (1 - d) = K (\operatorname{tr} \epsilon^e) \mathbf{I} + 2G \epsilon_D^e$$

$$\frac{d\epsilon^v}{dt} = \sqrt{\frac{3}{2}} A \exp\left(-\frac{Q}{RT}\right) \left(\frac{\tilde{\sigma}_D}{\sigma_{ref}}\right)^m \frac{\tilde{\sigma}_D}{\|\sigma_D\|}$$

$$\frac{d\epsilon^p}{dt} = \dot{\lambda}^p \frac{\partial g^p}{\partial \tilde{\sigma}}$$

$$f^p = \left[ (1-q_h) \left( \frac{\tilde{\sigma}_D}{3\sigma_c} + \frac{\tilde{\sigma}_m}{\sigma_c} \right)^2 + \frac{\tilde{\sigma}_D}{\sigma_c} \right]^2 + m_0 q_h^2 \left( \frac{\tilde{\sigma}_D}{3\sigma_c} + \frac{\tilde{\sigma}_m}{\sigma_c} \right) - q_h^2$$

$$q_h = \frac{R_p(\epsilon^p, \epsilon^v)}{[1 + (\alpha \Delta T)^n]^{(1-\frac{1}{n})}}, \quad \tilde{\sigma}_m = \frac{1}{3} \operatorname{tr}(\tilde{\sigma}), \quad \tilde{\sigma}_D = \sqrt{\frac{3}{2} \tilde{\sigma}_D : \tilde{\sigma}_D}$$

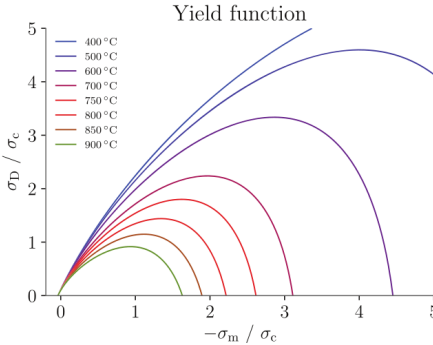
cf. Parisio, Lehmann und Nagel 2020

**Captured effects/phenomena:**

- elastic-plastic model with yield surface
- scalar internal damage variable  $d$
- temperature-dependent Young modulus
- Norton creep law with Arrhenius term

## EXAMPLARY SIMULATION RESULTS

**Yield function:**

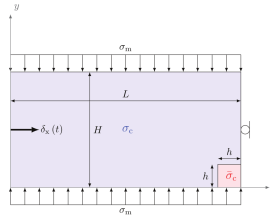


**Captured effects/phenomena:**

- temperature-dependent yield surface
- transition from dilatant to contractant plastic flow
- suitable for basaltic materials
- diffuse and localized damage possible

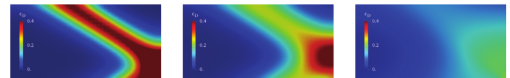
## EXAMPLARY SIMULATION RESULTS

### Test setting:

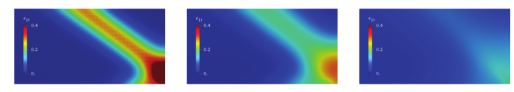


with localization nucleus

### Parameter study:



(a)  $T = 400^\circ\text{C}, \sigma_m = -50 \text{ MPa}$  (b)  $T = 600^\circ\text{C}, \sigma_m = -50 \text{ MPa}$  (c)  $T = 800^\circ\text{C}, \sigma_m = -50 \text{ MPa}$



(d)  $T = 400^\circ\text{C}, \sigma_m = -150 \text{ MPa}$  (e)  $T = 600^\circ\text{C}, \sigma_m = -150 \text{ MPa}$  (f)  $T = 800^\circ\text{C}, \sigma_m = -150 \text{ MPa}$



(g)  $T = 400^\circ\text{C}, \sigma_m = -250 \text{ MPa}$  (h)  $T = 600^\circ\text{C}, \sigma_m = -250 \text{ MPa}$  (i)  $T = 800^\circ\text{C}, \sigma_m = -250 \text{ MPa}$



(j)  $T = 400^\circ\text{C}, \sigma_m = -350 \text{ MPa}$  (k)  $T = 600^\circ\text{C}, \sigma_m = -350 \text{ MPa}$  (l)  $T = 800^\circ\text{C}, \sigma_m = -350 \text{ MPa}$

## CONSTITUTIVE EQUATIONS AND INTERPRETATION

Model including two creep mechanisms with different physical origin:

$$\begin{aligned}\dot{\epsilon}^{\text{cr}} &= \sqrt{\frac{3}{2}} A_1 e^{-Q_1/(RT)} \left( \frac{\bar{\sigma}}{\sigma_{\text{ref}}} \right)^m \frac{\sigma_D}{\|\sigma_D\|} + \sqrt{\frac{3}{2}} \frac{A_2}{D^3} e^{-Q_2/(RT)} \left( \frac{\bar{\sigma}}{\sigma_{\text{ref}}} \right) \frac{\sigma_D}{\|\sigma_D\|} \\ &= \sqrt{\frac{3}{2}} A_1 e^{-Q_1/(RT)} \left( \frac{\bar{\sigma}}{\sigma_{\text{ref}}} \right)^m \frac{\sigma_D}{\|\sigma_D\|} + \frac{3}{2} \frac{A_2}{\sigma_{\text{ref}} D^3} e^{-Q_2/(RT)} \sigma_D\end{aligned}$$

cf. Bérest u. a. 2019

Captured effects/phenomena:

- dislocation creep (power law)
- pressure-solution creep (linear law) involving (mean) grain size  $D$
- based on micromechanics and new experiments

## CONSTITUTIVE EQUATIONS AND INTERPRETATION

Model including two creep mechanisms with different physical origin:

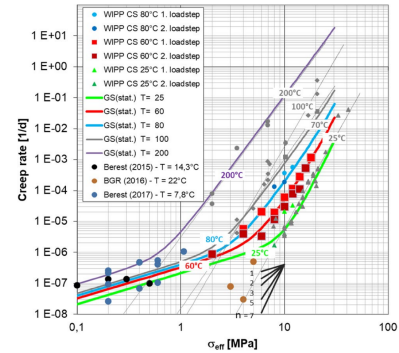
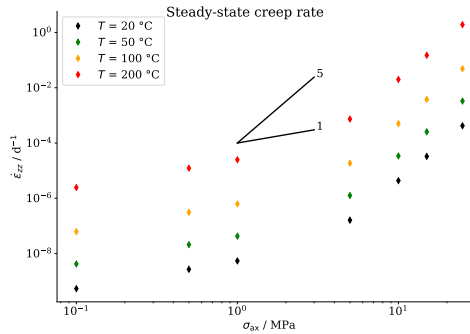
$$\begin{aligned}\dot{\epsilon}^{\text{cr}} &= \sqrt{\frac{3}{2}} A_1 e^{-Q_1/(RT)} \left( \frac{\bar{\sigma}}{\sigma_{\text{ref}}} \right)^m \frac{\sigma_D}{\|\sigma_D\|} + \sqrt{\frac{3}{2}} \frac{A_2}{D^3} e^{-Q_2/(RT)} \left( \frac{\bar{\sigma}}{\sigma_{\text{ref}}} \right) \frac{\sigma_D}{\|\sigma_D\|} \\ &= \sqrt{\frac{3}{2}} A_1 e^{-Q_1/(RT)} \left( \frac{\bar{\sigma}}{\sigma_{\text{ref}}} \right)^m \frac{\sigma_D}{\|\sigma_D\|} + \frac{3}{2} \frac{A_2}{\sigma_{\text{ref}} D^3} e^{-Q_2/(RT)} \sigma_D\end{aligned}$$

cf. Bérest u. a. 2019

Captured effects/phenomena:

- dislocation creep (power law)
- pressure-solution creep (linear law) involving (mean) grain size  $D$
- based on micromechanics and new experiments

## EXAMPLARY SIMULATION RESULTS



- steady state creep rate curve shows two distinct ranges
- importance of pressure-solution creep in *low-stress* environments
- dominance of dislocation creep at *high stresses*
- extrapolation with exponent from high creep rates would lead to wrong result
- temperature elevation increases both strain rates

# CONSTITUTIVE EQUATIONS AND INTERPRETATION

## Basic equations:

$$\dot{\epsilon}_{\text{cr}} = \dot{\epsilon}_{\text{cr}}^V + \dot{\epsilon}_{\text{cr}}^E + \dot{\epsilon}_{\text{cr}}^{\text{dam}}$$

$$\dot{\epsilon}_{\text{cr}} = A_p \frac{(\bar{\sigma}/\sigma_{\text{ref}})^{n_p}}{(\epsilon_0^V + \epsilon_{\text{cr}}^V)^{\mu_p}} \quad \text{with} \quad \bar{\sigma} = \sqrt{\frac{3}{2} \|\boldsymbol{\sigma}_D\|}$$

$$\dot{\epsilon}_{\text{cr}}^E = \sum_{i=1}^2 A_{s,i} \exp\left(-\frac{Q_i}{RT}\right) \left(\frac{\bar{\sigma}}{\sigma_{\text{ref}}}\right)^{n_i}$$

$$\dot{\epsilon}_{\text{cr}}^{\text{dam}} = \dot{\epsilon}_{\text{dil}} = A_1(\sigma_3) + A_2(\sigma_3) \exp[A_3(\sigma_3) U_{\text{dil}}] \dot{U}_{\text{dil}}$$

$$\text{with } U_{\text{dil}} = \int \langle \bar{\sigma} - \bar{\sigma}_{\text{dil}} \rangle d\epsilon_{\text{cr}}$$

cf. R. Günther und Salzer 2012; R. M. Günther  
u. a. 2015

## Captured effects/phenomena:

- inelastic behavior
- strain hardening creep law for total strain
- brittle-ductile transition
- primary, secondary and tertiary creep
- $\dot{\epsilon}_{\text{cr}}^{\text{dam}}$  as internal variable
- $\sigma_3$  as least compressive principal stress

## CONSTITUTIVE EQUATIONS AND INTERPRETATION

### Basic equations:

$$\dot{\epsilon}_{\text{cr}} = \dot{\epsilon}_{\text{cr}}^V + \dot{\epsilon}_{\text{cr}}^E + \dot{\epsilon}_{\text{cr}}^{\text{dam}}$$

$$\dot{\epsilon}_{\text{cr}} = A_p \frac{(\bar{\sigma}/\sigma_{\text{ref}})^{n_p}}{(\epsilon_0^V + \epsilon_{\text{cr}}^V)^{\mu_p}} \quad \text{with} \quad \bar{\sigma} = \sqrt{\frac{3}{2} \|\boldsymbol{\sigma}_D\|}$$

$$\dot{\epsilon}_{\text{cr}}^E = \sum_{i=1}^2 A_{s,i} \exp\left(-\frac{Q_i}{RT}\right) \left(\frac{\bar{\sigma}}{\sigma_{\text{ref}}}\right)^{n_i}$$

$$\dot{\epsilon}_{\text{cr}}^{\text{dam}} = \dot{\epsilon}_{\text{dil}} = A_1(\sigma_3) + A_2(\sigma_3) \exp[A_3(\sigma_3) U_{\text{dil}}] \dot{U}_{\text{dil}}$$

$$\text{with } U_{\text{dil}} = \int \langle \bar{\sigma} - \bar{\sigma}_{\text{dil}} \rangle d\epsilon_{\text{cr}}$$

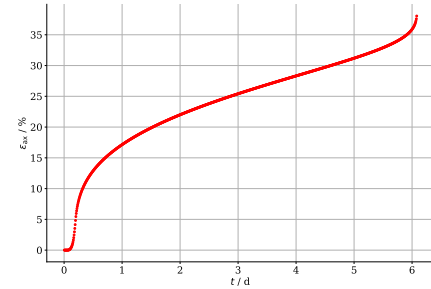
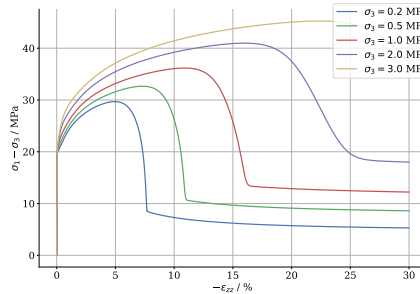
cf. R. Günther und Salzer 2012; R. M. Günther

u. a. 2015

### Captured effects/phenomena:

- inelastic behavior
- strain hardening creep law for total strain
- brittle-ductile transition
- primary, secondary and tertiary creep
- $\dot{\epsilon}_{\text{cr}}^{\text{dam}}$  as internal variable
- $\sigma_3$  as least compressive principal stress

## EXEMPLARY SIMULATION RESULTS



Stress-strain curve for triaxial test (*left*), creep curve for  $\sigma_3 = 3$  MPa,  $\sigma_1 = 41$  MPa (*right*)

- stress-dependent softening with pronounced peak stress → extreme ductility: no failure
- smooth transition from primary to secondary over to tertiary creep
- no (complicated) yield surface involved

# CONSTITUTIVE EQUATIONS AND INTERPRETATION

## Basic equations:

$$\boldsymbol{\sigma} = \mathbf{D} \cdot (\boldsymbol{\epsilon} - \boldsymbol{\epsilon}_p) ,$$

$$f = q^2 + Mp(p - p_c) \leq 0 \quad \text{with}$$

$$q = \sqrt{\frac{3}{2} \boldsymbol{\sigma}_D : \boldsymbol{\sigma}_D} , \quad p = -\frac{1}{3} \text{tr}(\boldsymbol{\sigma}) ,$$

$$\dot{\boldsymbol{\epsilon}}_p = \dot{\lambda}_p \, \mathbf{n} \quad \text{with} \quad \mathbf{n} = \frac{\mathbf{m}}{\|\mathbf{m}\|} , \quad \mathbf{m} = \frac{\partial f}{\partial \boldsymbol{\sigma}} ,$$

$$\dot{p}_c = -\dot{\epsilon}_p^V \left( \frac{1+e}{\lambda - \kappa} \right) p_c \quad \text{with} \quad \dot{\epsilon}_p^V \equiv \text{tr}(\dot{\boldsymbol{\epsilon}}_p) ,$$

$$\dot{p} = -\dot{\epsilon}_e^V \left( \frac{1+e}{\kappa} \right) p \quad \text{not used here!}$$

cf. Borja und Lee 1990; Callari, Auricchio und Sacco 1998

## Captured effects/phenomena:

- elasto-plastic deformation
- irreversible (plastic) pore compaction  
→ pressure-dependent plastic flow
- hardening and softening depending on consolidation
- critical state line (CSL)
- different loading and unloading stiffness
- originally without cohesion (can be considered)  
→ tension states problematic

# CONSTITUTIVE EQUATIONS AND INTERPRETATION

## Basic equations:

$$\boldsymbol{\sigma} = \mathbf{D} \cdot (\boldsymbol{\epsilon} - \boldsymbol{\epsilon}_p) ,$$

$$f = q^2 + Mp(p - p_c) \leq 0 \quad \text{with}$$

$$q = \sqrt{\frac{3}{2} \boldsymbol{\sigma}_D : \boldsymbol{\sigma}_D} , \quad p = -\frac{1}{3} \text{tr}(\boldsymbol{\sigma}) ,$$

$$\dot{\boldsymbol{\epsilon}}_p = \dot{A}_p \mathbf{n} \quad \text{with} \quad \mathbf{n} = \frac{\mathbf{m}}{\|\mathbf{m}\|} , \quad \mathbf{m} = \frac{\partial f}{\partial \boldsymbol{\sigma}} ,$$

$$\dot{p}_c = -\dot{\epsilon}_p^v \left( \frac{1+e}{\lambda - \kappa} \right) p_c \quad \text{with} \quad \dot{\epsilon}_p^v \equiv \text{tr}(\dot{\boldsymbol{\epsilon}}_p) ,$$

$$\dot{p} = -\dot{\epsilon}_e^v \left( \frac{1+e}{\kappa} \right) p \quad \text{not used here!}$$

## Captured effects/phenomena:

- elasto-plastic deformation
- irreversible (plastic) pore compaction  
→ pressure-dependent plastic flow
- hardening and softening depending on consolidation
- critical state line (CSL)
- different loading and unloading stiffness
- originally without cohesion (can be considered)  
→ tension states problematic

cf. Borja und Lee 1990; Callari, Auricchio und Sacco 1998

# CONSTITUTIVE EQUATIONS AND INTERPRETATION

## Basic equations:

$$\boldsymbol{\sigma} = \mathbf{D} \cdot (\boldsymbol{\epsilon} - \boldsymbol{\epsilon}_p) ,$$

$$f = q^2 + Mp(p - p_c) \leq 0 \quad \text{with}$$

$$q = \sqrt{\frac{3}{2} \boldsymbol{\sigma}_D : \boldsymbol{\sigma}_D} , \quad p = -\frac{1}{3} \text{tr}(\boldsymbol{\sigma}) ,$$

$$\dot{\boldsymbol{\epsilon}}_p = \dot{A}_p \mathbf{n} \quad \text{with} \quad \mathbf{n} = \frac{\mathbf{m}}{\|\mathbf{m}\|} , \quad \mathbf{m} = \frac{\partial f}{\partial \boldsymbol{\sigma}} ,$$

$$\dot{p}_c = -\dot{\epsilon}_p^V \left( \frac{1+e}{\lambda - \kappa} \right) p_c \quad \text{with} \quad \dot{\epsilon}_p^V \equiv \text{tr}(\dot{\boldsymbol{\epsilon}}_p) ,$$

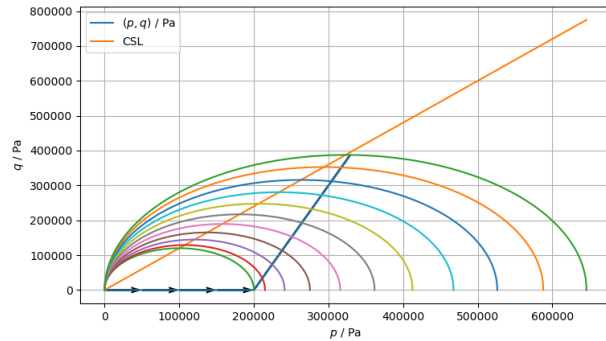
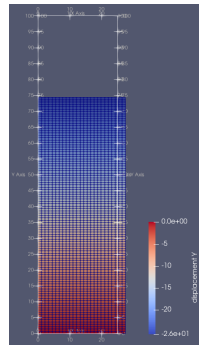
$$\dot{p} = -\dot{\epsilon}_e^V \left( \frac{1+e}{\kappa} \right) p \quad \text{not used here!}$$

cf. Borja und Lee 1990; Callari, Auricchio und Sacco 1998

## Captured effects/phenomena:

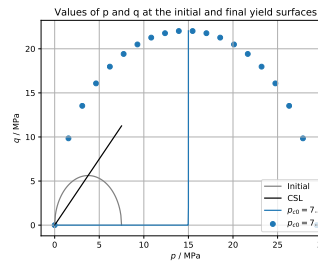
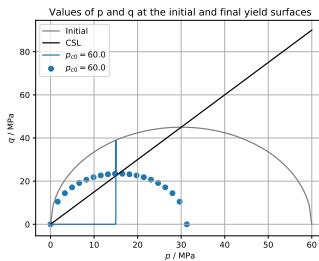
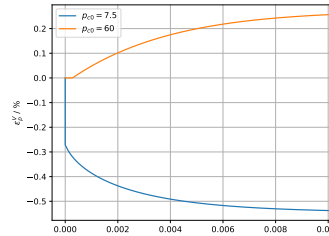
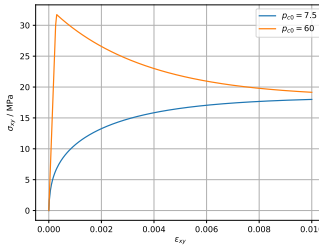
- elasto-plastic deformation
- irreversible (plastic) pore compaction  
→ pressure-dependent plastic flow
- hardening and softening depending on consolidation
- critical state line (CSL)
- different loading and unloading stiffness
- originally without cohesion (can be considered)  
→ tension states problematic

## TRIAXIAL BENCHMARK RESULTS



- setting (*left*) and stress trajectory with evolving yield surfaces as well as the CSL (*right*)
- stress trajectory approaches the CSL (when reached no resistance to plastic flow!)

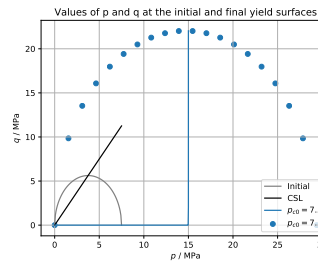
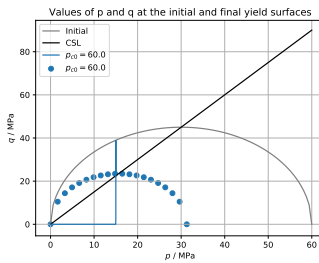
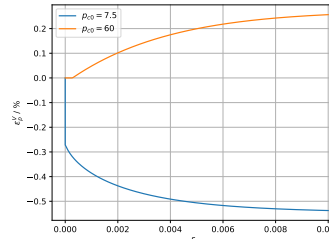
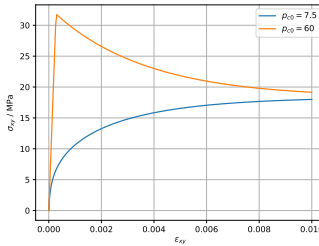
## PLANE STRAIN SIMPLE SHEAR TEST USING MTEST



Two different initial states:

- $p_{c0} \uparrow$ : dense/compacted soil
  - $p_{c0} \downarrow$ :  $p_{c0}$  loosened initial state
- same (asymptotic) critical state by
- softening (dilatancy) or
  - hardening (contraction)

# PLANE STRAIN SIMPLE SHEAR TEST USING MTEST



Two different initial states:

- $p_{c0} \uparrow$ : dense/compacted soil
  - $p_{c0} \downarrow$ :  $p_{c0}$  loosened initial state
- same (asymptotic) critical state by
- softening (dilatancy) or
  - hardening (contraction)

## TOTAL IMPLICIT SOLUTION SCHEME

Discretized set of equations (residuals for Newton-Raphson scheme)

$$\begin{aligned} \mathbf{f}_{\epsilon_e} &= \Delta\epsilon_e + \Delta\Lambda_p \mathbf{n} - \Delta\epsilon = \mathbf{0} , \\ f_{\Lambda_p} &= q^2 + M^2(p^2 - p p_c) = 0 , \\ f_{p_c} &= \Delta p_c + \Delta\epsilon_p^\vee \vartheta(\phi) p_c = 0 , \\ f_\phi &= \Delta\phi - (1 - \phi)\Delta\epsilon^\vee = 0 , \end{aligned}$$

Functional dependencies for the Jacobian

$$\begin{aligned} \mathbf{f}_{\epsilon_e} &= \mathbf{f}_{\epsilon_e}(\Delta\epsilon_e, \Delta\Lambda_p, \Delta p_c) , \\ f_{\Lambda_p} &= f_{\Lambda_p}(\Delta\epsilon_e, \Delta p_c) , \\ f_{p_c} &= f_{p_c}(\Delta\epsilon_e, \Delta\Lambda_p, \Delta p_c, \Delta\phi) , \\ f_\phi &= f_\phi(\Delta\phi) . \end{aligned}$$

## SEMI-EXPLICIT SOLUTION AND NUMERICAL REFINEMENT

- $\phi$  usually does not significantly change during the strain increment  $\rightarrow$  explicit update

$${}^{k+1}\phi = 1 - (1 - {}^k\phi) \exp(-\Delta\epsilon^V) . \quad (1)$$

- Normalize all residuals to similar order of magnitude (e. g. as strains)

$$f_{A_p} = f/\hat{f} = \{q^2 + M^2(p^2 - p p_c)\} / (E p_{c0}) . \quad (2)$$

- directly normalize the independent variable  $p_c$   $\rightarrow$  new reduced integration variable

$$p_c^r := p_c / \hat{p}_c = p_c / p_{c0} . \quad (3)$$

- add small value  $p_{amb}$  to the pressure for non-zero initial elastic range, i. e.

$$p := -I_1(\sigma)/3 + p_{amb} . \quad (4)$$

- limit the decrease of  $p_c$  to some minimal pre-consolidation pressure  $p_c^{min}$  with

$$\dot{p}_c = -\dot{\epsilon}_p^V \vartheta(e) (p_c - p_c^{min}) \quad \text{with} \quad p_c|_{t=0} = p_{c0} . \quad (5)$$

## SEMI-EXPLICIT SOLUTION AND NUMERICAL REFINEMENT

- $\phi$  usually does not significantly change during the strain increment  $\rightarrow$  explicit update

$${}^{k+1}\phi = 1 - (1 - {}^k\phi) \exp(-\Delta\epsilon^V) . \quad (1)$$

- Normalize all residuals to similar order of magnitude (e. g. as strains)

$$f_{A_p} = f/\hat{f} = \{q^2 + M^2(p^2 - p p_c)\} / (E p_{c0}) . \quad (2)$$

- directly normalize the independent variable  $p_c$   $\rightarrow$  new reduced integration variable

$$p_c^r := p_c / \hat{p}_c = p_c / p_{c0} . \quad (3)$$

- add small value  $p_{amb}$  to the pressure for non-zero initial elastic range, i. e.

$$p := -I_1(\sigma)/3 + p_{amb} . \quad (4)$$

- limit the decrease of  $p_c$  to some minimal pre-consolidation pressure  $p_c^{min}$  with

$$\dot{p}_c = -\dot{\epsilon}_p^V \vartheta(e) (p_c - p_c^{min}) \quad \text{with} \quad p_c|_{t=0} = p_{c0} . \quad (5)$$

## SEMI-EXPLICIT SOLUTION AND NUMERICAL REFINEMENT

- $\phi$  usually does not significantly change during the strain increment  $\rightarrow$  explicit update

$${}^{k+1}\phi = 1 - (1 - {}^k\phi) \exp(-\Delta\epsilon^V) . \quad (1)$$

- Normalize all residuals to similar order of magnitude (e. g. as strains)

$$f_{A_p} = f/\hat{f} = \{q^2 + M^2(p^2 - p p_c)\} / (E p_{c0}) . \quad (2)$$

- directly normalize the independent variable  $p_c$   $\rightarrow$  new reduced integration variable

$$p_c^r := p_c / \hat{p}_c = p_c / p_{c0} . \quad (3)$$

- add small value  $p_{amb}$  to the pressure for non-zero initial elastic range, i. e.

$$p := -I_1(\sigma)/3 + p_{amb} . \quad (4)$$

- limit the decrease of  $p_c$  to some minimal pre-consolidation pressure  $p_c^{min}$  with

$$\dot{p}_c = -\dot{\epsilon}_p^V \vartheta(e) (p_c - p_c^{min}) \quad \text{with} \quad p_c|_{t=0} = p_{c0} . \quad (5)$$

## SEMI-EXPLICIT SOLUTION AND NUMERICAL REFINEMENT

- $\phi$  usually does not significantly change during the strain increment  $\rightarrow$  explicit update

$${}^{k+1}\phi = 1 - (1 - {}^k\phi) \exp(-\Delta\epsilon^V) . \quad (1)$$

- Normalize all residuals to similar order of magnitude (e. g. as strains)

$$f_{A_p} = f/\hat{f} = \{q^2 + M^2(p^2 - p p_c)\} / (E p_{c0}) . \quad (2)$$

- directly normalize the independent variable  $p_c$   $\rightarrow$  new reduced integration variable

$$p_c^r := p_c / \hat{p}_c = p_c / p_{c0} . \quad (3)$$

- add small value  $p_{amb}$  to the pressure for non-zero initial elastic range, i. e.

$$p := -I_1(\sigma)/3 + p_{amb} . \quad (4)$$

- limit the decrease of  $p_c$  to some minimal pre-consolidation pressure  $p_c^{min}$  with

$$\dot{p}_c = -\dot{\epsilon}_p^V \vartheta(e) (p_c - p_c^{min}) \quad \text{with} \quad p_c|_{t=0} = p_{c0} . \quad (5)$$

## SEMI-EXPLICIT SOLUTION AND NUMERICAL REFINEMENT

- $\phi$  usually does not significantly change during the strain increment  $\rightarrow$  explicit update

$${}^{k+1}\phi = 1 - (1 - {}^k\phi) \exp(-\Delta\epsilon^V) . \quad (1)$$

- Normalize all residuals to similar order of magnitude (e. g. as strains)

$$f_{A_p} = f/\hat{f} = \{q^2 + M^2(p^2 - p p_c)\} / (E p_{c0}) . \quad (2)$$

- directly normalize the independent variable  $p_c$   $\rightarrow$  new reduced integration variable

$$p_c^r := p_c / \hat{p}_c = p_c / p_{c0} . \quad (3)$$

- add small value  $p_{amb}$  to the pressure for non-zero initial elastic range, i. e.

$$p := -I_1(\sigma)/3 + p_{amb} . \quad (4)$$

- limit the decrease of  $p_c$  to some minimal pre-consolidation pressure  $p_c^{min}$  with

$$\dot{p}_c = -\dot{\epsilon}_p^V \vartheta(e) (p_c - p_c^{min}) \quad \text{with} \quad p_c|_{t=0} = p_{c0} . \quad (5)$$

## IMPLEMENTATION INTO MFRONT

### Parameters and state variables

```
// environmental parameters (default values)
@Parameter stress p0 = 1e+3; //Pa
@PhysicalBounds p0 in [0:*[;
p0.setEntryName("AmbientPressure");

// material parameters
@MaterialProperty stress young;
@PhysicalBounds young in [0:*[;
young.setGlossaryName("YoungModulus");

...
@StateVariable real lp;
lp.setGlossaryName("EquivalentPlasticStrain");
@IntegrationVariable strain rpc;
@AuxiliaryStateVariable stress pc;
pc.setEntryName("PreConsolidationPressure");
@AuxiliaryStateVariable real phi;
phi.setGlossaryName("Porosity");
```

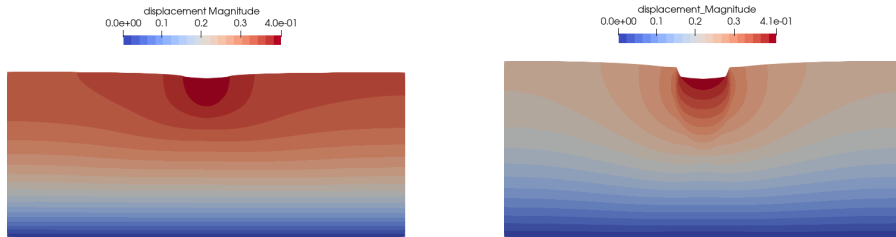
## IMPLEMENTATION INTO MFRONT

### Solution steps

```
@InitLocalVariables{
    //elastic predictor step
}
@Integrator{
    //plastic corrector step
}
@UpdateAuxiliaryStateVariables{
    //explicit porosity update
}
```

## GEOTECHNICAL EXAMPLE: FOUNDATION PROBLEM

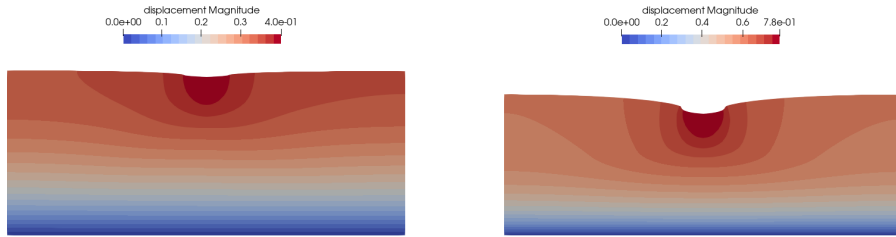
pure Von-Mises plasticity (*left*) versus Mohr-Coulomb model (*right*)



- Von-Mises plasticity as a *very special case* of some undrained geomaterial
- Mohr-Coulomb model shows particular failure kinematics

## GEOTECHNICAL EXAMPLE: FOUNDATION PROBLEM

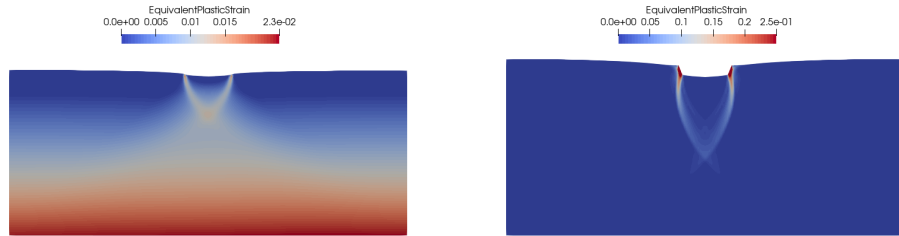
pure Von-Mises plasticity (*left*) versus Modified Cam clay model (*right*)



- Von-Mises plasticity as a reference (*very special case* of some undrained geomaterial)
- Modified Cam clay model shows plastic compaction at the base

## GEOTECHNICAL EXAMPLE: FOUNDATION PROBLEM

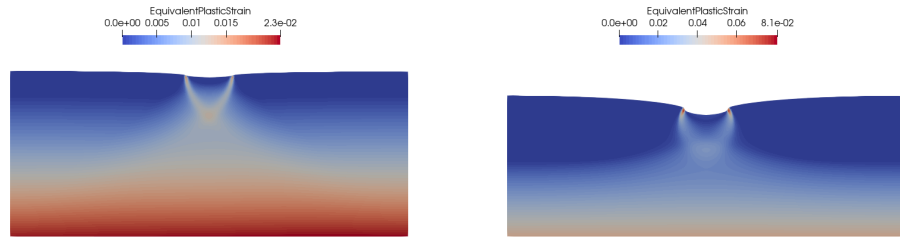
pure Von-Mises plasticity (*left*) versus Mohr-Coulomb model (*right*)



- Von-Mises plasticity as a reference (*very special case* of some undrained geomaterial)
- Mohr-Coulomb model shows particular failure kinematics

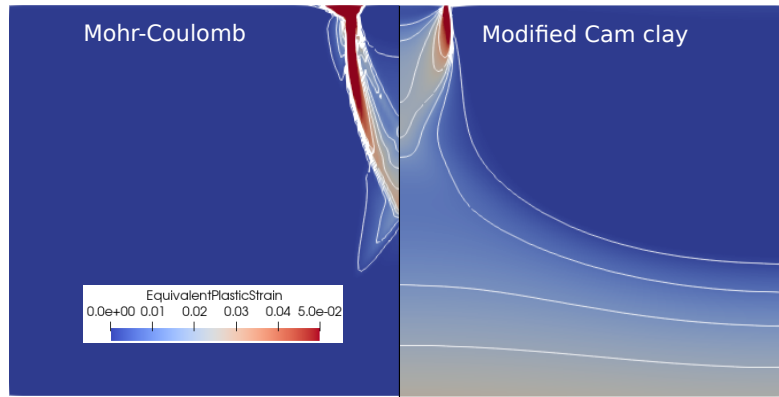
## GEOTECHNICAL EXAMPLE: FOUNDATION PROBLEM

pure Von-Mises plasticity (*left*) versus Modified Cam clay model (*right*)



- Von-Mises plasticity as a *very special case* of some undrained geomaterial
- Modified Cam clay model shows plastic compaction at the base

## GEOTECHNICAL EXAMPLE: FOUNDATION PROBLEM



- Mohr-Coulomb model: failure mechanism with localized slip
- Modified Cam clay model: load distributed, more diffuse "failure"

## POSSIBLE EXTENSIONS

- strong softening can cause mesh-dependent FE solution
  - regularization of localization
- need for stability enhancement (tensional states)
  - extension to Cohesive Cam clay model Gaume u. a. 2018
- extension to temperature-dependent soil behavior (permafrost)
- purely explicit implementation into *MFront* using  $\dot{f}_{A_p} = 0$

## ACKNOWLEDGMENTS

Merci beaucoup !

We are grateful to our funding agencies.

Many thanks to the great MFront and OpenGeoSys developer teams!



## LITERATURE

- [1] Pierre Bérest u. a. „Very Slow Creep Tests on Salt Samples“. In: *Rock Mechanics and Rock Engineering* 52.9 (2019), S. 2917–2934. ISSN: 1434453X. DOI: 10.1007/s00603-019-01778-9. URL: <http://dx.doi.org/10.1007/s00603-019-01778-9>.
- [2] Ronaldo I. Borja und Seung R. Lee. „Cam-Clay plasticity, Part 1: Implicit integration of elasto-plastic constitutive relations“. In: *Computer Methods in Applied Mechanics and Engineering* 78.1 (Jan. 1990), S. 49–72. ISSN: 00457825. DOI: 10.1016/0045-7825(90)90152-C. URL: <https://linkinghub.elsevier.com/retrieve/pii/004578259090152C>.
- [3] C. Callari, F. Auricchio und E. Sacco. „A finite-strain cam-clay model in the framework of multiplicative elasto-plasticity“. In: *International Journal of Plasticity* 14.12 (1998), S. 1155–1187. ISSN: 07496419. DOI: 10.1016/S0749-6419(98)00050-3.

## LITERATURE II

- [4] J. Gaume u. a. „Dynamic anticrack propagation in snow“. In: *Nature Communications* 9.1 (2018). ISSN: 20411723. DOI: 10.1038/s41467-018-05181-w. URL: <http://dx.doi.org/10.1038/s41467-018-05181-w>.
- [5] R Günther und K Salzer. „Advanced strain-hardening approach“. In: *Mechanical Behaviour of Salt VII* December 2016 (2012). DOI: 10.1201/b12041-4.
- [6] R. M. Günther u. a. „Steady-State Creep of Rock Salt: Improved Approaches for Lab Determination and Modelling“. In: *Rock Mechanics and Rock Engineering* 48.6 (2015), S. 2603–2613. ISSN: 07232632. DOI: 10.1007/s00603-015-0839-2.
- [7] Francesco Parisio, Christoph Lehmann und Thomas Nagel. „A Model of Failure and Localization of Basalt at Temperature and Pressure Conditions Spanning the Brittle-Ductile Transition“. In: *Journal of Geophysical Research: Solid Earth* 125.11 (2020), S. 1–18. ISSN: 21699356. DOI: 10.1029/2020JB020539.